Proceedings of the ASME 2010 3rd Joint US-European Fluids Engineering Summer Meeting and 8th International Conference on Nanochannels, Microchannels, and Minichannels
FEDSM-ICNMM2010
August 1-5, 2010, Montreal, Canada

FEDSM-ICNMM2010-30057

HYDROELASTIC STABILITY OF FLEXIBLE PANEL: EIGEN-ANALYSIS AND TIME-DOMAIN RESPONSE

Ben H. Tan
Fluid Dynamics Research Group
Curtin University of Technology
Perth, WA 6845
Australia
E-mail:benhoea.tan@postgrad.curtin.edu.au

Anthony D. Lucey
Fluid Dynamics Research Group
Curtin University of Technology
Perth, WA 6845
Australia
E-mail:A.Lucey@curtin.edu.au

Mark. W. Pitman
Fluid Dynamics Research Group
Curtin University of Technology
Perth, WA 6845
Australia
E-mail:M.Pitman@curtin.edu.au

ABSTRACT

A state-space model, based upon computational modeling, is used to investigate the hydroelastic stability of a finite flexible panel interacting with a uniform flow. A merit of this approach is that it allows the fluid-structure system eigenmodes to be found readily when structural inhomogeneity is included or a source of external excitation is present. The system studied herein is two-dimensional although the concepts presented can be readily extended to three dimensions. Two problems are considered. In the first, we solve the initial-value, boundary-value, problem to show how the system response evolves from a source of localized excitation. This problem is deceptively complex and has evidenced some very unusual behaviour as demonstrated by theoretical studies based on the assumption of an infinitely long flexible panel. Our contribution herein is to formulate and illustrate the use of a hybrid of theoretical and computational models that includes the effects of finiteness. In the second problem we solve the boundary-value problem to determine the long-time response and investigate the effects of adding localized structural inhomogeneity on the linear stability of a flexible panel. It is well known that a simple flexible plate first loses its stability to divergence that is replaced by modal-coalescence flutter at higher speeds. Our contribution is to show how the introduction of localized structural inhomogeneity can be used to modify the divergence-onset and flutter-onset critical flow speeds.

INTRODUCTION

This paper addresses and extends the classical fluid-structure interaction (FSI) problem wherein a flexible panel is destabilized by the action of a fluid flow parallel to the undisturbed panel; see Fig. 1. This FSI system is representative of many engineering applications; the interaction of the panels comprising the external skin of aircraft or ships with the adjacent flow is a common example. The high Reynolds number regime typical of these applications makes the neglect of viscous effects on the flow a good approximation. Accordingly, potential flow is most often assumed as is the case in this study. Given the importance and ubiquity of applications, this FSI system has generated a rich literature in which, most commonly, a Galerkin method is used to predict the system response with a particular focus on the parameters for which it becomes unstable. Thus, for example, [1-4], show that as the flow speed is increased for a given flexible plate, the panel first loses its stability to divergence. This buckling type of instability occurs because the fluid forces generated by a deformation exceed the restorative structural forces of that deformation. The fundamental is the critical mode for divergence. If the flow speed is increased further, divergence is replaced by modal-coalescence flutter that is best characterized as a Kelvin-Helmhotz resonance. Using a more versatile modeling approach [5], the engineering goal of this paper is to show how the introduction of localized structural inhomogeneity can be used to postpone the onset of divergence.

Clearly, the aforementioned boundary-value studies predict the long-time response of the system after transients from some form of initial excitation have either been attenuated or convected away. The finite-time response can be of equal importance in that it links the original source and characteristics of an initial deformation to the long-time response through a process of response evolution. The ability to model the finite-time, or receptivity, problem may lead to engineering strategies that interrupt or modify this evolution and thereby prevent or postpone panel instability. Studies of system response to a source of initial or continuing localized excitation have been presented. For example, [6] and [7] respectively used initial impulse and oscillatory line excitation for the present system, while [8] tackled the closely related shell problem with oscillatory line excitation. Using a different analytical approach, [9] showed that absolute instability – that aligns with divergence - could exist in the system if structural damping were included. However, these analyses assumed an infinitely long flexible panel and focused on the long-time response. Nevertheless, they showed that the system could support a remarkable range of FSI wave types. Using numerical simulation, [10] showed that the effects of finiteness and transients led to unstable responses unseen in the analyses of infinitely long elastic panels. Thus, the second goal of this paper is to extend the hybrid of theoretical and computation methods developed in [5] so as to be able to assemble the transient response of finite flexible panels in terms of system eigenmodes.

The paper is laid out as follows. We first extend the FSI system model of [5] to permit the inclusion of impulse line excitation and a supporting spring foundation that may be either uniform or comprise a discrete spring at some point along the flexible plate. We then briefly illustrate how our model is able to model transient responses; however, we do not present a comprehensive investigation of this problem herein. The major results of this paper that follow pertain to the long-time response of simple panels. These focus on the effects of structural inhomogeneity as a means of postponing the critical flow speed at which hydroelastic instability, most particularly divergence, sets in.

METHODS

Our methods extend the modeling of [5] in which the Laplace equation for the perturbation-velocity potential is solved using a boundary-element method fully coupled to a finite-difference representation of classical thin-plate mechanics. A single system equation was derived in terms of the interfacial deflection, $\eta(x,t)$, and its time derivatives which could then be cast in time-invariant state-space form and thus permitted the extraction of the system eigenmodes. For the present investigation of long-time response, we modify the structural side of the equation to permit the incorporation of structural inhomogeneity.

For the initial-value problem we extend the governing state-space equation to include a forcing vector; this can be used to model the response to any of an impulse, step function or continuous sinusoidal excitation Alternatively, an initial condition such as enforced initial surface curvature can be applied to which the system responds. The SIMO (single input multiple output) state-space model is then used to investigate the eigenmodes and transient response of the system.

In Fig. 1, P_e is a pressure disturbance acting at the i-th collocation point of the structure surface where $x=(i/N)L$ and L is the panel length discretized into N elements. P_e can be viewed as a form of external disturbance to the system. In the case of an impulse

$$\mathrm{I} = \int P_e \, \delta x \, dt \tag{1}$$

where P_e is the magnitude of the pressure pulse, δx is the streamwise extent of the panel on which it acts and the integral is taken over the time during which the pulse is applied.

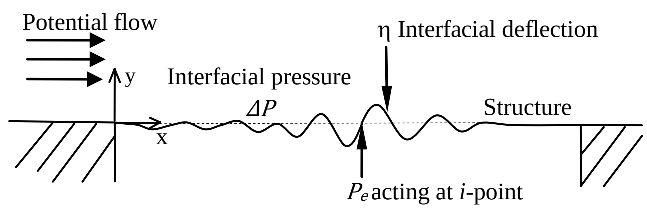

FIGURE 1. SCHEMATIC OF THE FLUID-STRUCTURE SYSTEM STUDIED

The fluid pressure perturbation experienced by the wall is found by solving the Laplace equation for the perturbation potential. A source-sink singularity boundary-element is used, having first discretized the interface into the set of N elements (or panels). The strength of the singularities is determined by the enforcement of the kinematic (or no-flux) boundary condition at the fluid-solid interface. The perturbation potential, Φ, can then be written in terms of the interfacial deflection, $\eta(x,t)$. Finally, the linearized unsteady Bernoulli equation is used to determine the pressure perturbation along the interface. Full details of this method are documented in [5] and [11]. The resulting pressure perturbation in the discretized system is then given as

$$-\{\Delta P\} = 2\rho[\Phi][D^+]\{\ddot{\eta}\} + (2\rho U_\infty[T][D^+] + 2\rho U_\infty[\Phi][D_1])\{\dot{\eta}\} + 2\rho {U_\infty}^2[T][D_1]\{\eta\} \tag{2}$$

where $[\Phi]$ and $[T]$ are matrices of invariant influence coefficients that arise from the boundary-element deployed, $[D^+]$ and $[D_1]$ are spatially averaging and differentiation matrices, and ρ and U_∞ are the density and mean speed of the fluid; the over-dot notation on the interfacial variable indicates differentiation with respect to time.

For the structural side of the system, a spring-backed flexible-plate model is used [12]. Here, the mass times acceleration of material points of the wall results from the action of the flexural and spring forces generated by the wall deformation, together with fluid loading, $-\{\Delta P\}$, and the externally applied excitation, $\{P_e\}$. Cast in finite-difference form, using the same discretisation that defined the panels in the flow solution, the FSI-system equation is therefore

$$\rho_m h[I]\{\ddot{\eta}\} + d[I]\{\dot{\eta}\} + (B[D_4] + K[I])\{\eta\} = -\{\Delta P\} + \{P_e\} \qquad (3)$$

where,

$$\{P_e\} = \begin{Bmatrix} \vdots \\ p_e \\ \vdots \end{Bmatrix}$$

and where ρ_m ,h and B are respectively, the density, thickness and flexural rigidity of the flexible plate, K is the coefficient of the uniform spring foundation, d is the coefficient of a dashpot type of damping in the structure, and $[I]$ and $[D_4]$ are respectively, the identity and fourth-order spatial differentiation matrices.

By substituting the interfacial fluid pressure of Eqn. (2) into Eqn. (3), and re-arranging, we obtain

$$[A]\{\ddot{\eta}\} + [B]\{\dot{\eta}\} + [C]\{\eta\} = -\{P_e\} \qquad (4)$$

where

$$[A] = -\rho_m h[I] + 2\rho[\Phi][D^+]$$
$$[B] = -d[I] + 2\rho U_\infty[T][D^+] + 2\rho U_\infty[\Phi][D_1]$$
$$[C] = -B[D_4] - K[I] + 2\rho {U_\infty}^2[T][D_1]$$

Re-arranging Eqn. (4) so that the left-hand side is the acceleration term gives,

$$\{\ddot{\eta}\} = -[A]^{-1}[B]\{\dot{\eta}\} - [A]^{-1}[C]\{\eta\} - [A]^{-1}\{P_e\} \qquad (5)$$

We now define $[E] = -[A]^{-1}[B]$ and $[F] = -[A]^{-1}[C]$, so that Eqn. (5) becomes

$$\{\ddot{\eta}\} = [E]\{\dot{\eta}\} + [F]\{\eta\} - [A]^{-1}\{P_e\} \qquad (6)$$

Introducing state variables $x_i = \eta_i$ and $x_{N+i} = \dot{\eta}_i$ for i from 1st point to the Nth point, the $2N$ output vector for the state-space model is

$$\begin{Bmatrix} \{\eta\} \\ \{\dot{\eta}\} \end{Bmatrix} = \{x\} \qquad \text{or} \qquad \begin{Bmatrix} \{\eta\} \\ \{\dot{\eta}\} \end{Bmatrix} = [\mathrm{I}]\{x\} \qquad (7)$$

Using these definitions, Eqn. (6) is then converted into the state differential equation

$$\{\dot{x}\} = \begin{bmatrix} 0 & \mathrm{I} \\ F & E \end{bmatrix}\{x\} - \begin{bmatrix} 0 & 0 \\ 0 & A^{-1} \end{bmatrix}\begin{Bmatrix} 0 \\ \{P_e\} \end{Bmatrix} \qquad (8)$$

and letting

$$[G] = -\begin{bmatrix} 0 \\ i^{th}\ column\ of\ [A]^{-1} \end{bmatrix} \text{ and } [H] = \begin{bmatrix} 0 & \mathrm{I} \\ F & E \end{bmatrix}$$

noting that vector G is of length $2N$ and matrix H is $2N$ x $2N$, the final form of the state differential Eqn. (8) is

$$\{\dot{x}\} = [H]\{x\} + [G]p_e \qquad (9)$$

In the absence of continuing excitation, the long-time response is found by first assuming single-frequency response in the time domain, and then extracting the resulting eigenvalues of $[H]$. The system eigenvectors can then be used to assemble the deflection, $\eta(x,t)$, of the panel.

To solve for the transient response to a form of external excitation, the Laplace transform of Eqn. (9) is taken. Re-arranging gives

$$X(s) = [sI - H]^{-1}X(0) + [sI - H]^{-1}Gp_e(s) \qquad (10)$$

where $X(s)$ is the transform of the state-space vector. We note that $[sI - H] = \Psi(s)$ is the Laplace transform of state transition matrix $\Psi(t) = \exp(Ht)$.
Taking the inverse Laplace transform of Eqn. (10), we obtain

$$X(t) = \exp(Ht)\,x(0) + \int_0^t exp[H(t-\tau)]Gp_e(\tau)d\tau \qquad (11)$$

or

$$X(t) = \Psi(t)x(0) + \int_0^t \Psi(t-\tau)Gp_e(\tau)d\tau$$

Once the initial condition $x(0)$, the input $p_e(\tau)$ and the state transition matrix $\Psi(t)$ are known, the time response of $x(t)$ can be numerically evaluated. This matrix-inversion approach is convenient for low-order systems.

For higher-order systems, there are several other methods for evaluating the state transition matrix in closed form. Instead of solving the two main Eqns. (2)-(3) by finite-differences in the time domain, we apply a zero-order hold on our input Eqn. (8) to make the system digital. This gives the time-domain continuous system (H,G). So we can use the relationship $t=kT$ to transform the state-space solution into a sampled system with a sampling time T. To implement this approach we use MATLAB to compute the transient responses. The MATLAB function **lsim** is used to simulate a continuous system with a specified input. This function works by calling the **c2d**, which converts the system (H, G) into the equivalent discrete system. Once the system model is discretized, the function is used to simulate discrete-time systems with the specified input. Because of this, simulation programs like MATLAB are subjected to round-off errors associated with the discretization process that are similar to finite-differencing errors in the time domain.

RESULTS

Complex flexible panel: divergence-onset prediction and transient response

Here we consider a spring-backed flexible plate that approximates a compliant wall of the type investigated in [5,12,13]. The properties of this wall have h=0.01m, ρ_m=852kg/m^3, B=4.44x10^{-2}Nm^2, d=20000Ns/m^3 and K=3.68x10^{7}N/m^3; the length, L, of the flexible panel is 0.6m and the fluid is water with density ρ =1000kg/m^3. However, for greater generality and following [13], we present our results using a non-dimensional flow speed, or flow-to-wall stiffness ratio, defined as

$$\Lambda^I = 3\pi^3\rho\frac{{U_\infty}^2}{(3BK^3)^{\frac{1}{4}}} \tag{12}$$

By applying the state-space model and setting the forcing term to zero, the eigenvalues and eigenmodes are calculated. Figs. 2(a) and 2(b) show the variation of the 40 eigenvalues closest to origin with flow-to-wall stiffness ratio Λ^I. In this calculation, the wall was discretized into N=800 elements and all $2N=1,600$ system eigenvalues are computed to determine the point of divergence-onset accurately; this is the value of Λ^I at which a positive (amplifying) part to the real part of the eigenvalue appears in Fig. 2(a).

Carpenter & Garrad [12] derived analytical expressions for the divergence-onset flow speed and the wavelength of the critical divergence mode. By assuming the wall to be of infinite extent they used a travelling–wave approach for all system disturbances. Divergence-onset flow speed, U_D, and critical wavelength, λ_D, were given respectively by

$$U_D = 2\left(\frac{BK^3}{27\rho^4}\right)^{1/8} \quad \text{and} \quad \lambda_D = 2\pi\left(\frac{3B}{K}\right)^{1/4} \tag{13a,b}$$

Using the wall properties above in these analytical expressions gives a value of U_D that, when non-dimensionalized using Eqn. (12), yields a divergence-onset stiffness ratio of Λ^I=124.0. Our prediction of divergence-onset gives its value as just above 127 as can be seen in Fig. 2(a). Hence there is a difference of approximately 2.4% between the two approaches. Exact agreement could only be expected in the limit of infinite plate length and the present prediction for a plate of finite length is expected to be higher, as found, because of the structural restraints at its leading and trailing edges. This correlation serves to validate the integrity of our approach and its implementation.

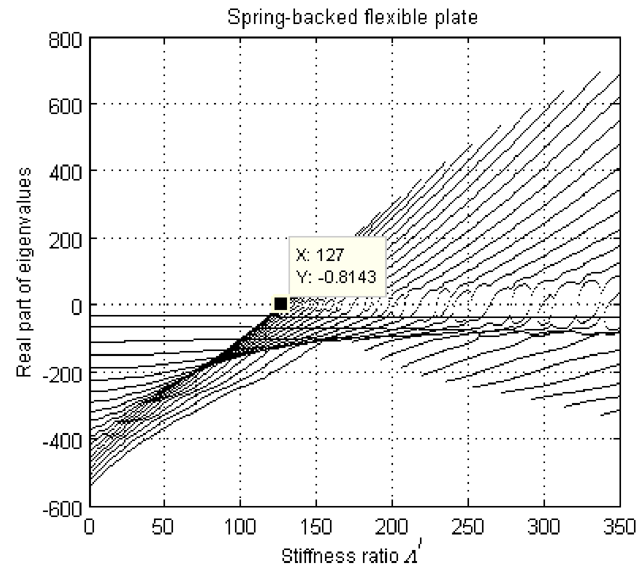

(a)

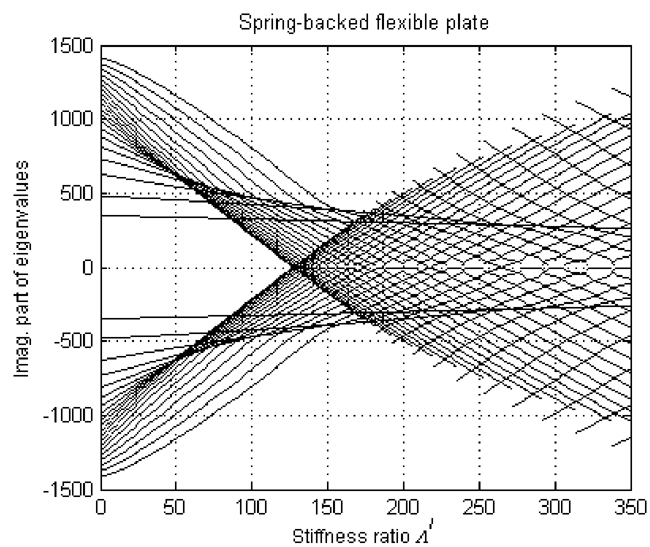

(b)

FIGURE 2. VARIATION OF SYSTEM EIGENVALUES WITH NON-DIMENSIONAL FLOW SPEED FOR A SPRING-BACKED FLEXIBLE PLATE, (a) IS THE REAL (POSITIVE, GROWTH; NEGATIVE, DECAY) PART, AND (b) IS THE IMAGINARY (OSCILLATORY) PART OF THE EIGENVALUES.

We now illustrate the application of our initial-value modeling of the system behavior that would lead to the long-time instability predicted above. Figs. 3(a) and 3(b) show the transient response of the compliant wall. A point impulse is applied at the centre of the panel to initiate motion. Fig. 3(a) shows the time sequence of wall deformations at the non-dimensional flow speed Λ^I=127, just below divergence onset, for the sequence of time steps 2ΔT, 3ΔT, 4ΔT and 50ΔT where

ΔT = 0.016. After the initial wave propagation from the impulse, the wall is seen to select the 12th mode shape that is the critical divergence mode at a slightly higher flow speed than that of divergence onset. Again, good agreement is found with the traveling-wave based predictions of [12]; Eqn. (13b) predicts a critical wavelength of 0.49 m that would yield close to 12 disturbance wavelengths on the present finite wall of length 0.6 m. After the wave has propagated outwards from the point of initial excitation, it then decays due to the effect of structural damping. At the much higher flow speed than that of divergence onset, represented by Λ^I= 350 used to generate Fig. 3(b), the wall is unstable. In this figure the sequence of time steps is 3ΔT, 5ΔT, 7ΔT and 9ΔT where ΔT = 0.255 ms. Rapid growth is seen to spread to both upstream and downstream of the point of initial excitation; this is characteristic of absolute instability in such systems [9,10].

Simple flexible panel: the effect of structural inhomogeneity on divergence onset

We now consider a panel comprising a simple elastic plate and show how the addition of a single (line) spring support affects its stability bounds. The dimensional properties used herein correspond to those of an aluminum panel of length L=0.6 m with h=0.0025 m, ρ_m=2600 kg/m^3 and B=76.62 Nm^2; the fluid is water with density ρ_f=1000 kg/m^3 Hinged-end restraints are applied to the panel. The spring constant is varied in the form of multiples of k where k=6x10^3 N/m^2. In the results that first follow we present the variation of system eigenmodes with a non-dimensional flow-speed parameter, Λ^F, based upon the flow-to-wall stiffness ratio for the basic panel. Thus

$$\Lambda^F = \rho \frac{{U_\infty}^2 L^3}{B} \tag{14}$$

Figs. 4(a) and 4(b) show the effect of adding a localized spring support at the panel mid-point on the long-time hydroelastic behavior of the flexible panel for the cases *0* (no spring), *6k* and *15k.* The variation of the (lowest-frequency) eigenmodes is plotted with Λ^F. For the standard homogeneous case (0k) divergence-onset is seen to occur at Λ^F=40 in Fig. 4(a) where the first appearance of a positive real part of the eigenvalue appears that commences the divergence loop of instability. This agrees well with the results of previous Galerkin-based analyses, for example [2-4]. As the spring constant, k, is increased, the critical value Λ^F and, hence, the divergence-onset flow speed for a panel of given flexural rigidity, is seen to increase. The modal-coalescence flutter that occurs at Λ^F-values higher than those of the divergence loop is also postponed to higher flow speeds; however, this effect is not as marked as the postponement of divergence. However, the latter suggests a simple strategy for extending the envelope of stable operation of fluid-loaded panels in engineering applications.

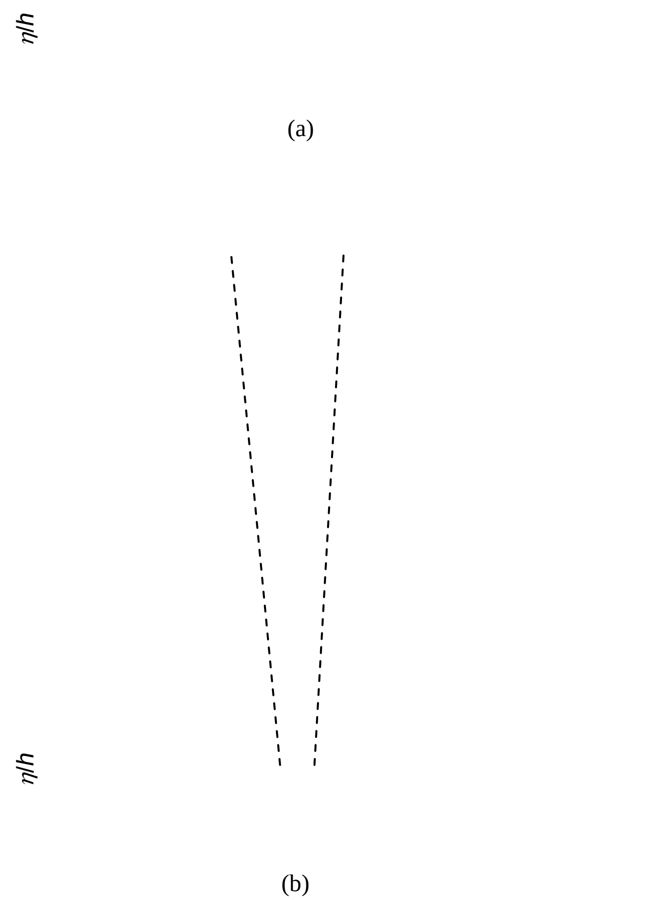

FIGURE 3. INSTANTANEOUS FLEXIBLE-WALL PROFILES DEVELOPING FROM AN IMPULSE: (a) MARGINALLY PRE-DIVERGE, (b) POST-DIVERGENCE.

We now show how the added spring contributes to the postponement of divergence in terms of energy budgets. The dimensional wall energy comprises three parts, namely its strain energy E_S, its kinetic energy E_K and its spring energy E_{SP}, respectively defined as follows

$$E_S = \frac{1}{2} B \int \eta_{,xx}^2 \, dx \tag{15}$$

$$E_K = \frac{1}{2} \rho_m h \int \eta_{,t}^2 \, dx \tag{16}$$

$$E_{SP} = \frac{1}{2} k \eta_i^2 \tag{17}$$

Lucey [10] also introduced a term called the virtual work done by the hydrodynamic stiffness component of the pressure in the establishment of a wall deformation. This is defined as

$$E_{VW} = -\frac{1}{2} \int \eta p\,(0,0,\eta) dx \tag{18}$$

The energy terms shown in Figs. 5(a) and 5(b) are normalised by dividing by the square of deflection amplitude A. Hence they become independent of amplitude.

It was shown in [10] that divergence onset can be defined as the flow speed for which E_{VW} exactly balances the mechanical energy of the wall. To show how this occurs, both without and with (for 6k) an added spring, we present Figs. 5(a) and 5(b). The first corresponds to the result for no added spring in Fig. 4 and is a time-stepping numerical evaluation of the energy terms for a stiffness ratio marginally lower than that of divergence onset at Λ^F=40. Because this value of Λ^F is so close to divergence at which the hydrodynamic stiffness balances the restorative stiffness, the wall acceleration and velocity are very small, hence the insignificant values of E_K in the plot and the very slow oscillation of the wall. The key feature of this plot is that E_{VW} is almost exactly balanced with the plate's strain energy, E_S. Fig. 5(b) is the equivalent result when a localized spring is included at the panel mid-point and corresponds to the result of Fig. 4 for 6k. The evaluation is conducted just before divergence onset at Λ^F=122. It is now seen that both the strain energy of the plate and the spring energy contribute to the value of total value of mechanical energy that balances E_{VW} and the proportions in which they do so. In this particular case, it is evident that the bulk of the wall's restorative force is provided by the added spring in the stabilisation strategy.

The extent to which the strategy of divergence postponement can be taken is now explored. Figs. 6(a) and 6(b) show the variation of system eigenvalues with stiffness ratio, Λ^F, that result when a very large multiple of k is used; the added spring is now so stiff as to be considered an additional restraint that fixes the wall displacement to be zero at its point of application. Contrasting these figures with those of Figs. 4(a) and 4(b), shows that a fundamental change in solution morphology occurs. In fact it is now the second system mode that first succumbs to divergence at approximately Λ^F=280. This could be anticipated because the effective restraint at the panel mid point divides the original into two panels each of length 0.5L. An approximate prediction using Eqn. (14) suggests that halving the length of the panel changes the critical value of Λ^F from 40 to 2^3 x 40 = 320. The actual value of 280 predicted by Fig. 4(a) is lower than 320 because there effectively exists two adjacent interacting flexible panels of length 0.5L as opposed to a single panel of the same length.

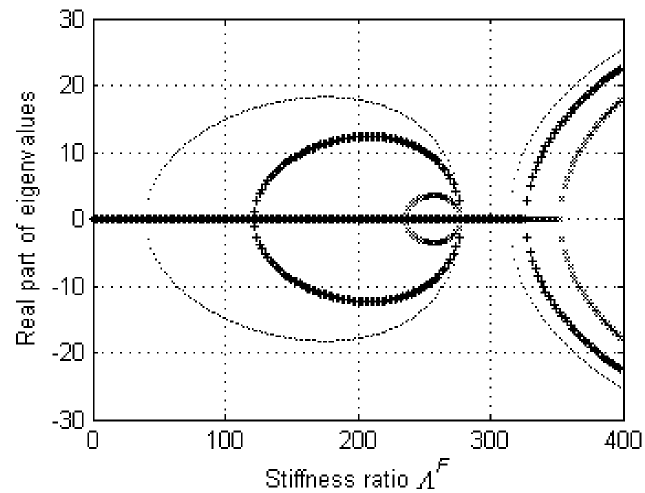

(a)

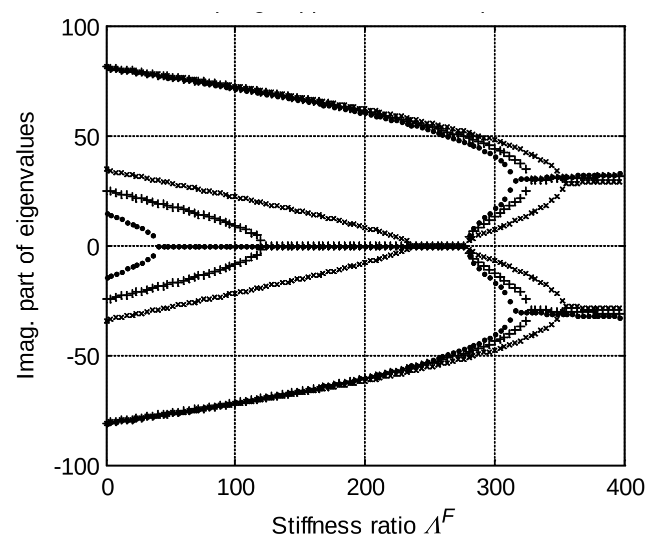

(b)

FIGURE 4. VARIATION OF SYSTEM EIGENMODES WITH NON-DIMENSIONAL FLOW SPEED FOR DIFFERENT VALUES OF LOCALIZED SPRING SUPPORT APPLIED AT PANEL MID-POINT: •, NONE; +, 6*k*; X, 15*k* WHERE (a) IS THE REAL (POSITIVE, GROWTH; NEGATIVE, DECAY) PART, AND (b) IS THE IMAGINARY (OSCILLATORY) PART OF THE EIGENVALUES.

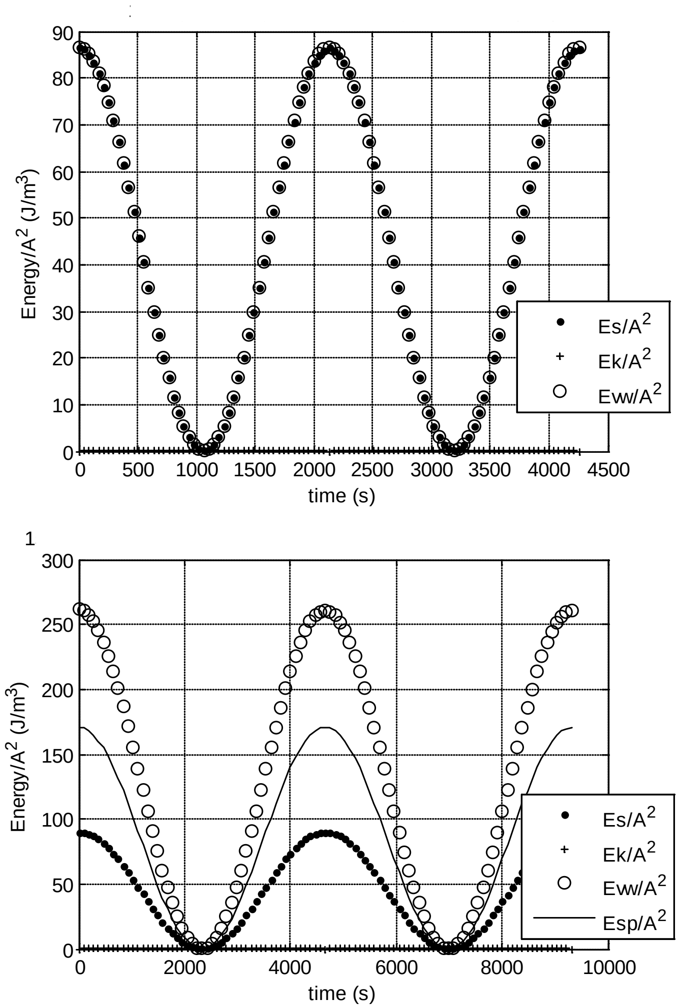

(b)

FIGURE 5. VARIATION OF STRAIN, KINETIC AND SPRING ENERGY, AND VIRTUAL WORK DONE BY THE HYDRODYNAMIC STIFFNESS, WITH TIME JUST BEFORE DIVERGENCE ONSET, FOR (a) HOMOGENEOUS FLEXIBLE PLATE, AND (b) FLEXIBLE PLATE WITH AN ADDED SPRING SUPPORT OF COEFFICIENT 6*k* INCLUDED AT THE PANEL MID-POINT.

Figs. 7(a) and 7(b) show the effect of moving the effective restraint of an infinitely stiff spring from the panel mid-point, as for Figs. 6(a) and 6(b), to a point a distance 0.25*L* from its leading edge. The solution morphology now resembles that of the base case of the simple flexible panel and represented by the results of Figs. 4(a) and 4(b). Compared to the base case, the effect of divergence postponement is seen to be less than that when the restraint is at the panel mid-point. This is to be expected because the critical mode for divergence is the fundamental that has maximum deflection at 0.5*L*. Placing the restraint at 0.25*L* again divides the panel with the critical value of Λ^F generated by the sub-panel of length 0.75*L*. Very careful inspection of the results in Fig. 7(a) show that a mild instability exists at values of Λ^F below that of divergence onset. This type of low-speed single-mode flutter was identified and its causes elucidated in [5]. In most engineering applications, it would be eliminated by even small amounts of structural damping present in a real panel.

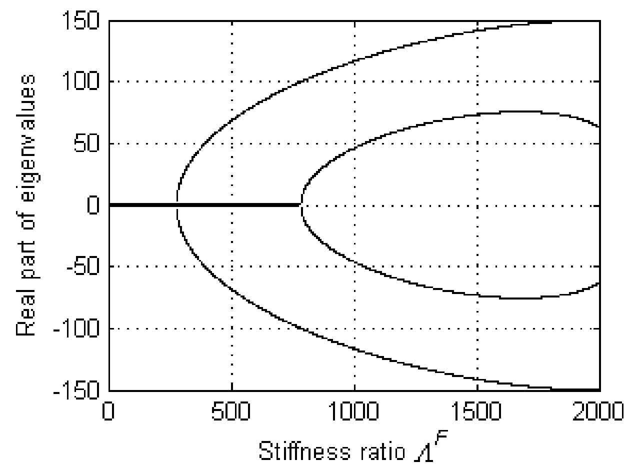

(a)

(b)

FIGURE 6. VARIATION OF SYSTEM EIGENMODES WITH NON-DIMENSIONAL FLOW SPEED FOR AN EFFECTIVELY INFINITELY STIFF SPRING ADDED AT PANEL MID-POINT WHERE (a) IS THE REAL (POSITIVE, GROWTH; NEGATIVE, DECAY) PART, AND (b) IS THE IMAGINARY (OSCILLATORY) PART OF THE EIGENVALUES.

Finally, we summarize the effects of finite spring stiffness on divergence-onset flow speed. To do this, we change the non-dimensionalization scheme from that of Eqn. (14) that scheme was based upon panel length. The foregoing results show the added spring can effectively shorten the panel length thus rendering this non-dimensional scheme inappropriate as a measure of divergence onset flow speed. Thus, we allow panel length to be a free parameter and non-dimensionalize using the scheme developed in [7] and elaborated in [14]. This gives

$$\overline{U} = U_{\infty}\frac{(\rho_m h)^{3/2}}{\rho B^{1/2}} \tag{19}$$

and a non-dimensional panel length

$$\overline{L} = \frac{L}{L_{ref}} \tag{20}$$

where

$$L_{ref} = \frac{\rho_m h}{\rho} \tag{21}$$

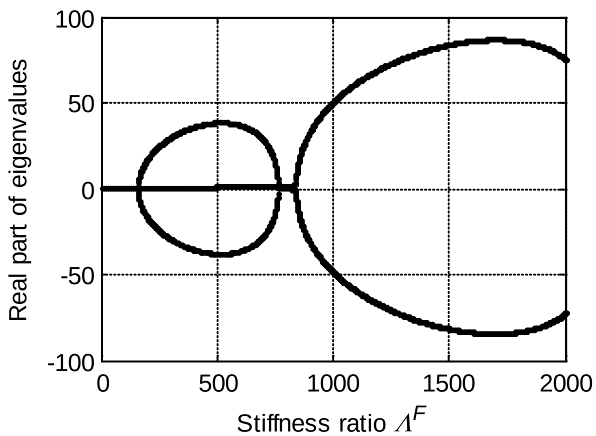

(a)

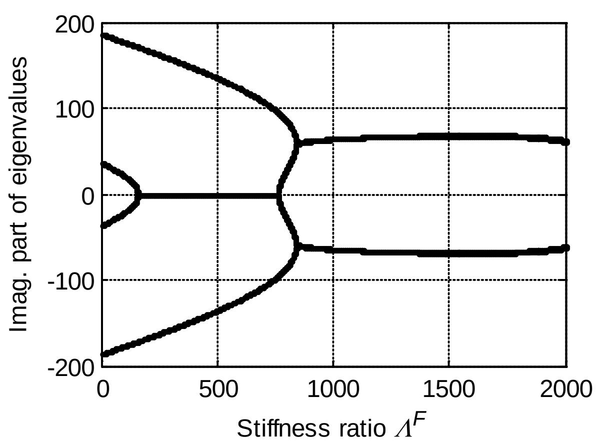

(b)

FIGURE 7. VARIATION OF SYSTEM EIGENMODES WITH NON-DIMENSIONAL FLOW SPEED FOR AN EFFECTIVELY INFINITELY STIFF SPRING ADDED TO THE PANEL AT A LOCATION 0.25*L* FROM THE LEADING EDGE, WHERE (a) IS THE REAL (POSITIVE, GROWTH; NEGATIVE, DECAY) PART, AND (b) IS THE IMAGINARY (OSCILLATORY) PART OF THE EIGENVALUES.

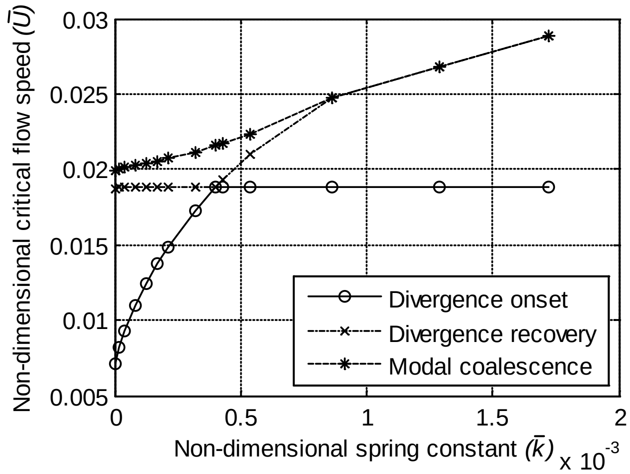

(a)

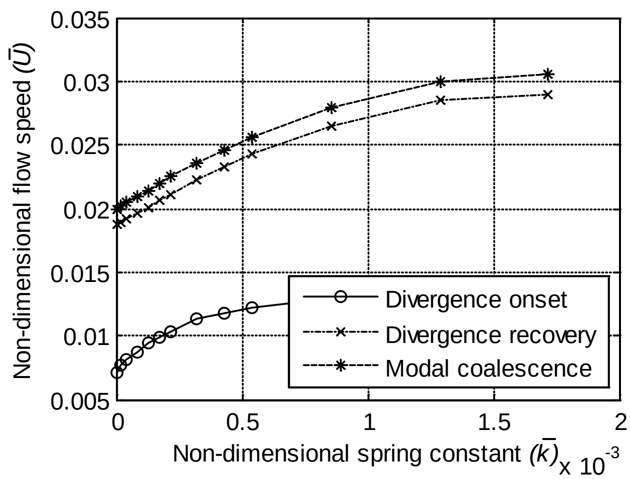

(b)

FIGURE 8. VARIATION OF DIVERGENCE-ONSET, DIVERGENCE-RECOVERY AND MODAL-COALESCENCE FLUTTER-ONSET FLOW SPEEDS WITH THE COEFFICIENT OF THE ADDED SPRING SUPPORT FOR A PANEL WITH LENGTH $\overline{L}$ = 92.3: SPRING ADDED AT (a) PANEL MID-POINT, AND (b) 0.25*L* FROM THE LEADING EDGE OF THE PANEL.

Clearly the relationship between the new non-dimensional flow speed and the non-dimensional stiffness ratio, Λ^F, is

$$\overline{U} = \sqrt{\frac{\Lambda^F}{\overline{L}^3}} \tag{22}$$

To complete the non-dimensional scheme, the coefficient of the added spring support is non-dimensionalized using the reference length of Eqn. (21) and the flexural rigidity of the plate. Thus for uniformly distributed and a single localized spring support respectively, we have

$$\bar{K} = \frac{K L_{ref}{}^4}{B} \quad \text{and} \quad \bar{k} = \frac{k L_{ref}{}^3}{B} \qquad (23a,b)$$

Thus, for the case of an isolated spring support, the non-dimensional divergence onset flow speed is functionally given as

$$\bar{U}_D = f(\bar{L}, \bar{k}, \bar{x}_k) \qquad (24)$$

where $\bar{x}_k = x_k/L$ is the non-dimensional distance of the location of the added spring from the panel leading edge.

Figs. 8(a) and 8(b) show the variation of divergence-onset flow speed with the magnitude of the added spring support for the two cases of spring location $\bar{x}_k$ =0.5 and 0.25; in each figure $\bar{L}$ =92.3 (that gives the same physical length as the panels investigated through Figs. 4-6). These results clearly show that the addition of a single localized spring support can significantly increase the divergence-onset flow speed. As could be expected on physical grounds, this strategy is more effective when the spring is placed at the panel mid-point. When placing it here, it is noted that there is a threshold of approximately $\bar{k}$ =0.4 x 10^{-3}, for which further stabilization of the system ceases. This is because the second system mode replaces the first as the critical mode for divergence onset. Thus, this value of $\bar{k}$ may be regarded as optimal for the design of divergence-free flexible panels.

CONCLUSIONS

A state-space model has been developed for predicting the aero-/hydro-elastic behavior of a flexible wall. The model fuses computational and theoretical methods exploiting the advantages of each. A particular merit of the approach is that it can be used to find the FSI eigenmodes of flexible panels and walls that include localized inhomogeneity. The model also permits the study of the initial-value problem so that the way a system response develops from some form of initial source of excitation can be charted.

In this paper, we have demonstrated how disturbances evolve for a spring-backed flexible-plate model of a compliant coating in the pre- and post-divergence regimes. For the latter, it is demonstrated that the instability is absolute and thereby spreads to all parts of the coating.

The results presented herein for a simple flexible panel show that the addition of an isolated spring support to the structure can yield a very significant extension to the flow-speed range before divergence instability sets in. It is also shown that, dependent upon the location of the added spring, an optimal value of spring stiffness coefficient exists. This type of tailored stabilization strategy may find engineering use in that it can be far more effective than a ‘brute force’ approach to design that, for example, thickens the entire panel to prevent aero-/hydro-elastic instability within the operating envelope of flow speeds.

REFERENCES

[1] Dugundji, J., Dowell, E. & Perkin, B., Subsonic flutter of panels on a continuous elastic foundation**,** *AIAA Journal* **1**, pp. 1146-1154, 1963.

[2] Weaver, D.S. & Unny, T.S., The hydroelastic stability of a flat plate. *ASME: Journal of Applied Mechanics* **37**, pp 823-827., 1971.

[3] Ellen, C.H., The stability of simply supported rectangular surfaces in uniform subsonic flow. *ASME: Journal of Applied Mechanics* **95**, pp 68-72., 1973.

[4] Lucey, A.D. & Carpenter, P.W., The hydroelastic stability of three-dimensional disturbances of a finite compliant panel. *Journal of Sound and Vibration* **165**, pp.527-552, 1993.

[5] Pitman, M.W.,& Lucey, A.D., On the direct determination of the eigenmodes of finite flow-structure systems. *Proceedings of the Royal Society A* **465**, 257-281, 2009.

[6] Brazier-Smith, P.R. & Scott, J.F., Stability of fluid flow in the presence of a compliant surface. *Wave Motion* **6**. pp 436-450, 1984.

[7] Crighton, D.G. & Oswell, J.E., Fluid loading with mean flow. I. Response of an elastic plate to localized excitation. *Philosophical Transactions of the Royal Society of London A*, **335**, pp. 557-592, 1991.

[8] Peake, N., On the behaviour of a fluid-loaded cylindrical shell with mean flow. *Journal of Fluid Mechanics* **338**, pp. 387-410, 1997.

[9] Abrahams, I.D. & Wickham, G.R., On transient oscillations of plates in moving fluids.*Wave Motion* **33**, pp. 7-23, 2001.

[10] Lucey, A.D., The excitation of waves on a flexible panel in a uniform flow. *Philosophical Transactions of the Royal Society of London A* **356**, pp. 2999-3039, 1998.

[11] Lucey, A.D. & Carpenter, P.W. A numerical simulation of the interaction of a compliant wall and inviscid flow. *Journal of Fluid Mechanics* 234, pp. 121-146, 1992.

[12] Carpenter, P.W. & Garrad A.D., The hydrodynamic stability of flows over Kramer-type compliant surfaces. Part 2. Flow-induced surface instabilities. *Journal of Fluid Mechanics* **170**, 199-232, 1986

[13] Lucey, A.D., Cafolla, G.J., Carpenter, P.W. & Yang, M. The nonlinear hydroelastic behaviour of flexible walls. *Journal of Fluids and Structures* **11**, pp. 717-744, 1997

[14] Lucey, A.D., Sen, P.K. & Carpenter, P.W. 2003 Excitation and evolution of waves on an inhomogeneous flexible wall in a mean flow. *Journal of Fluids and Structures* **18**, pp. 251-267, 2003